Metallopeptoid Helicates

International Edition: DOI: 10.1002/anie.201800583
German Edition: DOI: 10.1002/ange.201800583

Self-Assembled Cyclic Structures from Copper(II) Peptoids

*Totan Ghosh, Natalia Fridman, Monica Kosa, and Galia Maayan**

Abstract: *Metal–ligand coordination is a key interaction in the self-assembly of both biopolymers and synthetic oligomers. Although the binding of metal ions to synthetic proteins and peptides is known to yield high-order structures, the self-assembly of peptidomimetic molecules upon metal binding is still challenging. Herein we explore the self-assembly of three peptoid trimers bearing a bipyridine ligand at their C-terminus, a benzyl group at their N-terminus, and a polar group (N-ethyl-R) in the middle position (R = OH, OCH_3, or NH_2) upon Cu^{2+} coordination. X-ray diffraction analysis revealed unique, highly symmetric, dinuclear cyclic structure or aqua-bridged dinuclear double-stranded peptoid helicates, formed by the self-assembly of two peptoid molecules with two Cu^{2+} ions. Only the macrocycle with the highest number of intermolecular hydrogen bonds is stable in solution, while the other two disassemble to their corresponding monometallic complexes.*

Metal ions often play a crucial role in the structure and function of biopolymers, being employed in various tasks including folding, recognition, and catalysis. Some peptides exploit metal–ligand interactions to direct self-assembly towards the formation of nanostructures with unique conformations and functionalities.[1] Indeed, metal–ligand coordination is one of the most used interactions to drive the self-assembly of small molecules as well as of synthetic peptides and proteins into various 2D and 3D supramolecular architectures[2]—spanning from macrocycles and other geometrical shapes to cages and metal-organic frameworks (MOFs),[3] lattices,[4] discs, spherical shells or fibrils,[5] and additional quaternary structures.[5b,c] In recent years, a variety of oligomeric sequences akin to peptides, namely peptidomimetic foldamers,[6] capable of binding metal ions[7–9] have been developed, and some enabled biomimetic functions such as selective recognition,[10] allosteric cooperativity,[11] and catalysis.[12] An important class of peptidomimetic foldamers is peptoids—N-substituted glycine oligomers—which are capable of various applications such as metal binding,[9] catalysis,[12,13] and in medicine.[14] Peptoids can adopt stable secondary structures,[15] and self-assemble into sheets and nanotubes through hydrophobic interactions.[16] Macrocyclization of peptoids has also been demonstrated,[17] but to date could only be achieved by the formation of covalent bonds between pendant and/or backbone groups within the oligomer. Peptoids can be easily synthesized from primary amines on a solid support,[18] thereby resulting in highly versatile scaffolds. This synthesis enables the facile incorporation of various metal-binding ligands in different positions along the sequence, potentially triggering the self-assembly of these peptoids into well-defined supramolecular architectures upon metal coordination. However, despite decades of research in the fields of foldamers, peptidomimetics, and peptoids, the formation of 3D complex architectures by metal-coordination-driven self-assembly has not been reported. In the last few years, our group has focused on the synthesis and characterization of metal-binding peptoids bearing various chelating ligands[9a–b,10,19,20] as well as their metal-bound structures (metallopeptoids). These peptoids showed excellent biomimetic function, such as selective recognition[10] and cooperative catalysis;[12b–c] however, like other examples, their self-assembly into higher structures was limited. Herein we capitalize on our ability to form metallopeptoid duplexes (Scheme 1 a)[10] for the design of short peptoid sequences containing a bipyridine ligand (Bipy, Nbp), an ethanol group (Nhse), and a benzyl group (Npm) that can potentially self-assemble upon Cu^{2+} binding, while stabilizing metallopeptoid macrocycles through metal-oxo bridges (Scheme 1 b).

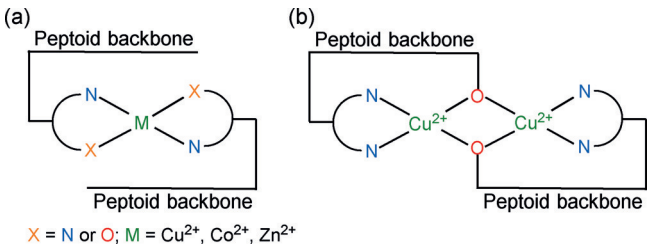

Scheme 1. Representation of metallopeptoid duplexes based on our previous work (a) and a designed metallopeptoid macrocycle (b).

Initially six peptoid trimers were synthesized by incorporating a bulky non-metal-binding group (benzyl, Npm) that should facilitate interaction between the Bipy and OH side chains,[12b] and by varying the positions of the three side chains with respect to one another (peptoids **1**–**6**, Figure S1). The peptoids were synthesized by the "submonomer" solid-phase method, cleaved from the solid support, and purified by high-performance liquid chromatography (HPLC; > 95 % purity). The molecular weight determined by electrospray mass spectrometry (ESIMS) was consistent with the mass expected for their sequences (see the Supporting Information). Each of the six oligomers (0.1 mmol) was dissolved in methanol (1 mL) and the solution was stirred for 10 min. These were further treated with 1 equiv of copper(II) perchlorate hexahydrate, and the mixtures were stirred for 24 h at room

[*] Dr. T. Ghosh, Dr. N. Fridman, Dr. M. Kosa, Prof. G. Maayan
Schulich Faculty of Chemistry
Technion-Israel Institute of Technology
Technion City, Haifa 3200008 (Israel)
E-mail: gm92@technion.ac.il

Supporting information and the ORCID identification number(s) for the author(s) of this article can be found under: https://doi.org/10.1002/anie.201800583.

temperature. From the six solution mixtures, the complex containing the sequence NpmNhseNbp (**3**) precipitated as a blue solid while the others failed to form stable complexes, probably because of coordination geometry considerations. This blue solid was isolated, washed, dried, and re-dissolved in acetonitrile. Slow evaporation led to shiny needle-like crystals being acquired after seven days. X-ray diffraction studies revealed the first high-resolution structure of a self-assembled metallocyclic peptoid to date (**7**, Figure 1).

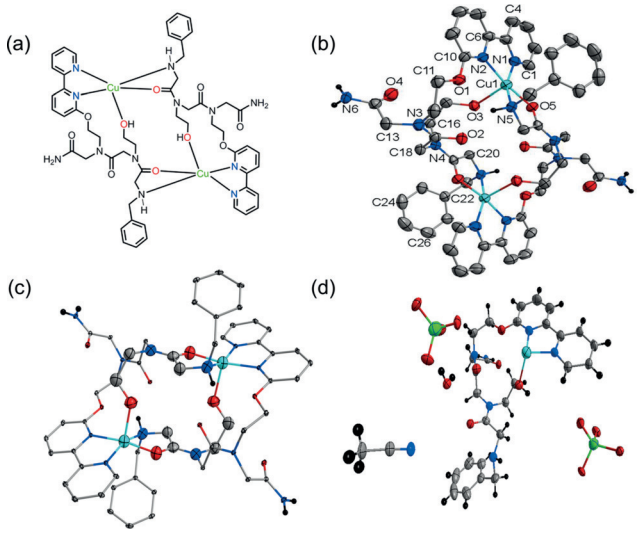

Figure 1. a) Chemdraw view of **7** and b) ORTEP view and the atom-numbering scheme for **7** without the counterions and solvent molecules. Thermal ellipsoids are drawn at the 50% probability level. c) ORTEP view for **7** to show the cyclic geometry. Thermal ellipsoids are drawn at the 50% probability level. All other atoms except the cycle are shown with 5% probability for clarity. d) ORTEP view of an asymmetric unit of the crystal.

Metallopeptoid **7** does not have the oxo bridges we envisioned (see Scheme 1 b), but is instead a highly symmetric macrocycle containing two Cu^{2+} ions bound to two peptoid molecules (Figure 1 a–c), in which every peptoid acts as a pentadentate ligand. Each metal center has an $\{N_3O_2\}$ environment consisting of: 1) two N atoms from the Bipy group (N1 and N2) and one oxygen atom from the -OH group (O3) of one peptoid molecule, and 2) one nitrogen atom and one oxygen atom from the terminal secondary amine (HN5) and its neighboring carbonyl group (O5) of the second peptoid molecule.

Pentacoordinated Cu^{2+} complexes usually adopt either a square-pyramidal (SP) or a trigonal-bipyramidal (TBP) geometry (or any of the distorted intermediate geometries). The distortion of the coordination environment from TBP to SP can be evaluated by the Addison distortion index τ, which is defined as $\tau = [\theta - \varphi/60]$, where θ and φ are the two largest coordination angles and $\tau = 0$ for a perfect SP geometry and 1 for an ideal TBP geometry.[21] In complex **7**, the calculated τ value for both Cu1 and Cu2 is 0.208, which clearly suggests a distorted SP geometry for each copper ion,[21a,22] and the distance between them is 6.805 Å. The two Bipy nitrogen atoms from one peptoid ligand and the carbonyl oxygen atom and terminal nitrogen atoms from the other peptoid ligand construct the square base of each of the two structurally similar copper atoms, while the OH group of the ethanolamine moiety occupies the apical position of the pyramid. The bond length between O3 (OH) and Cu1 (2.236 Å) is longer than the one between O5 (O=C) and Cu1 (1.987 Å) and also longer than the expected bond between Cu^{2+} and O^-, which is within the range of 1.87–1.98 Å.[23] From these data it is evident that there is only a weak interaction between O3 and Cu^{2+}, thus O3 remains protonated and is coordinated to Cu^{2+} as an -OH group. The substantial elongation of the axial Cu–O3(OH) bond compared to the equatorial Cu–N bonds is caused by the active Jahn–Teller distortion of the Cu^{2+} ion. The asymmetric unit of **7** consists of a [Cu(**3**)] unit with a lattice of two perchlorate ions, one acetonitrile molecule, and one water molecule (Figure 1 d), hence both Cu ions are in the +2 oxidation state. The two water molecules form hydrogen bonds with the oxygen atoms (O) of the amide carbonyl group, and the perchlorate anions assist in stabilizing the crystal through weak interactions with these water molecules. Additional crystallographic and geometrical parameters are summarized in Table S1.

Metallopeptoid **7** is highly soluble in acetonitrile and the dissolved crystals were further subjected to solution-phase analysis. Various MS studies, including high-resolution MS (HRMS) as well as computed and experimental isotopic envelope analysis, revealed a consistent mass of 584.1648, which corresponds to the mass of the monomeric complex **3**Cu (calcd Mw = 584.14). The mass of **7** was not obtained in these measurements, thus suggesting that the dicopper complex is not present in solution. The X-band EPR spectra of the dissolved crystals in acetonitrile solution, which was frozen at 180 K, clearly indicated the presence of Cu^{2+} ions, and the Hamiltonian parameters obtained from the simulation of the spectra were $g_{\parallel} = 2.210$, $g_{\perp} = 2.062$, and $A_{\parallel} = 159$ G (Figure S28a). These parameters, however, are in agreement with an $\{N_2O_2\}$ tetragonal coordination geometry,[24,9a] not the square-pyramidal geometry that was seen in the crystal-structure analysis, and could be explained by the presence of a monomeric complex, in which the Cu center is bound to two nitrogen atoms from the Bipy group, one oxygen atom from the ethanolic group, and one oxygen atom from a backbone carbonyl moiety. To further investigate the existence of the monomeric Cu^{2+}-peptoid complex in solution, we performed density functional theory (DFT) calculations (see the Supporting Information for details). The conformers **3**Cu and **3**Cu′ were optimized and verified as local minima, both in the gas phase and in acetonitrile solution (Tables S6–S8). Both structures include a distorted square-planar Cu complex, in which a Cu^{2+} ion binds the two nitrogen atoms from the Bipy group, one oxygen atom from the ethanolic group, and one oxygen atom from the backbone carbonyl group (Figure 2). This $\{N_2O_2\}$ tetragonal coordination geometry is in agreement with the Hamiltonian parameters obtained from the EPR spectra of **7**. Interestingly, the calculated **3**Cu complex has an intramolecular OH–N hydrogen bond between the OH and the secondary amine group (Figure 2 a, green circle). Overall the DFT calculations support the spectroscopic experimental data, thus indicating the existence of **3**Cu, rather than **7**, in

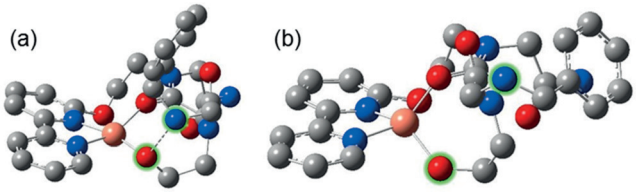

Figure 2. Optimized structure of the Cu peptoid in the gas phase or in acetonitrile solution, where both N and O are protonated (**3**Cu, a) or not protonated (**3**Cu′, b). The oxygen and nitrogen atoms forming the hydrogen bond in **3**Cu are highlighted in green, hydrogen atoms are omitted for clarity.

solution. It has previously been shown that metalloproteins and peptides crystallize as dimers and even as tetramers, while they are monomeric in solution.[25] It has also been demonstrated that the coordination of copper ion(s) to labile ligands, such as the NH group in the peptoid, can be easily replaced by coordinating solvent molecules, such as acetonitrile.[26] Moreover, when we allowed the solution of **3**Cu in acetonitrile to slowly evaporate, we recovered the crystals of complex **7**. We therefore propose that there exists a solid-state/solution equilibrium, in which the self-assembly process occurs only in the solid state.

At this point we wanted to investigate whether this self-assembly process can take place with similar peptoid trimers and chose to replace the ethanolic group by either a methoxy group (Nme) or an ethylamine group (Nae). Our hypothesis was that eliminating either the hydrogen bonding present in **3**Cu or the generation of a tetragonal $\{N_2O_2\}$ copper complex might disable the formation of monomeric complexes, thus also facilitating the stabilization of the dicopper complexes in solution. Accordingly, the peptoids NpmNmeNbp (**3A**) and NpmNaeNbp (**3B**) were prepared on a solid support, characterized, purified (>95%), and their identity was verified by MS. Both **3A** and **3B** were treated with 1 equiv of copper perchlorate in methanol followed by the addition of a solution of ammonium hexafluorophosphate in water. No precipitation was observed in either case, and the two blue solutions were left undisturbed for several days while the solvent was allowed to evaporate slowly. Shiny blue diamond-shaped crystals suitable for X-ray structure analysis were obtained after three days from the copper solution of **3A** (metallopeptoid **8**, Figure 3), while shiny deep-green triangular-shaped crystals were obtained after two days from the copper solution of **3B** (metallopeptoid **9**, Figure 4). X-ray structure analysis of these crystals revealed that both **8** and **9** are highly symmetric macrocycles, consisting of two Cu^{2+} ions bound to two peptoid molecules akin to **7**, but the new side chains were not involved in the coordination of copper. Instead, a bound water molecule provides an oxo bridge between the two copper ions and, therefore, each peptoid acts as a tetradentate ligand rather than a pentadentate ligand as in **7**.

A perspective ORTEP view with the atom-labeling scheme of complex **8** is presented in Figure 3. Additional crystallographic and geometrical parameters are summarized in Table S2. The asymmetric unit of **8** consists of a [{Cu(**3A**)}$_2$·H_2O] entity with a lattice of one perchlorate and three

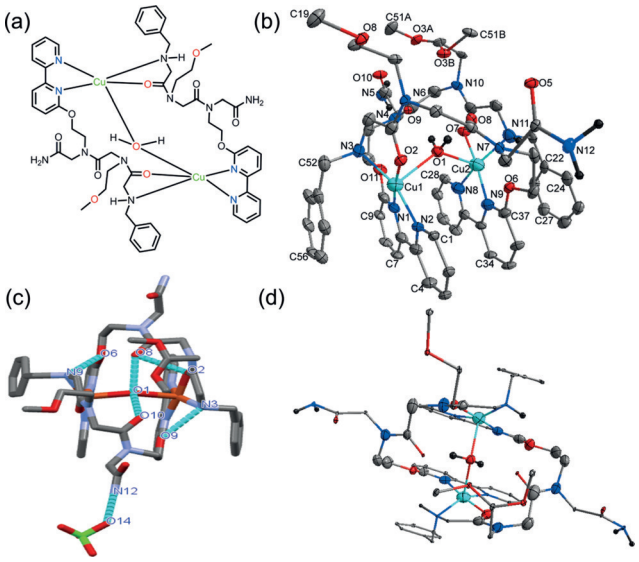

Figure 3. a) Chemdraw view of **8** and b) ORTEP view and the atom-numbering scheme for **8** without the counterions and solvent molecules. Thermal ellipsoids are drawn at the 50% probability level. c) 3D view of the crystal with hydrogen bonding (green dotted line). d) ORTEP view of **8** to show the cyclic geometry with a bridging water molecule. Thermal ellipsoids are drawn at the 50% probability level. All other atoms except the cycle are shown with 5% probability for clarity. Hydrogen atoms are also omitted for clarity.

hexafluoride phosphate ions. In the complex, each peptoid ligand coordinates to the metal center through its two Bipy nitrogen atoms, one carbonyl oxygen atom, and the N-terminus nitrogen atom. Both Cu^{2+} ions adopt a pentacoordination geometry, which is facilitated by the binding of one H_2O molecule between the two Cu^{2+} ions. The calculated τ values for Cu1 and Cu2 are 0.314 and 0.298, respectively, which suggests a distorted SP geometry for each copper ion. The two Bipy nitrogen atoms from one peptoid together with the carbonyl oxygen atom and terminal nitrogen atoms from the other peptoid ligand construct the square base of each of the two structurally similar copper atoms, while the bridging oxygen atom occupies the apical position of the pyramid. The substantial elongation of the axial Cu–OH_2 bonds [2.417(4) and 2.383(4) Å for Cu1 and Cu2, respectively] compared to the equatorial Cu–N bonds is caused by the active Jahn–Teller distortion of the Cu^{2+} ion. Within the Cu1-(O1)-Cu2 core, the Cu···Cu distance is 4.354 Å, which is much shorter than the one in **7**. The Cu1-O-Cu2 bond angle is 130.19(16), which is slightly larger than its ideal angle (120°). The bond angle of H-O-H is 105.75° and the O–H bond length in the water molecule is 0.99 Å; these values are almost the same as the values in a pure water molecule. The hydrogen atoms of the bridging water molecule form intramolecular hydrogen bonds with the nearest carbonyl oxygen atoms (O4 and O5) and the perchlorate ion stabilizes the crystal lattice through intermolecular hydrogen bonding with one terminal NH_2 group.

An ORTEP view of complex **9** with the atom-labeling scheme is presented in Figure 4. Additional crystallographic and geometrical parameters are summarized in Table S3. The asymmetric unit of **9** consists of a [{Cu(**3B**)}$_2$·H_2O] unit with

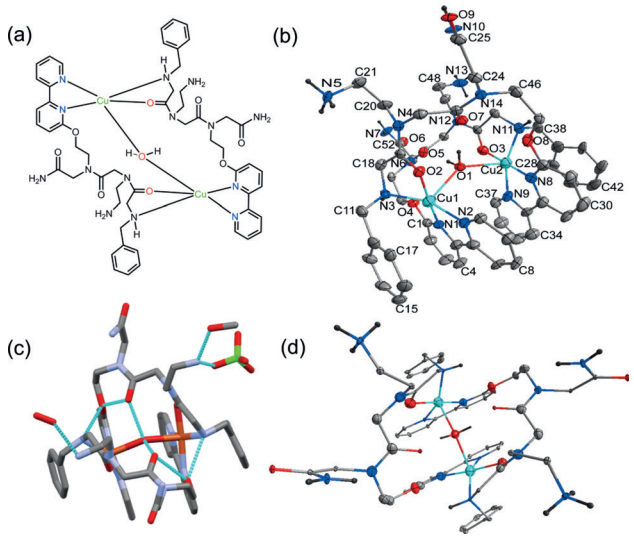

Figure 4. a) Chemdraw view of **9** and b) ORTEP view and the atom-numbering scheme for **9** without the counterions and solvent molecules. Thermal ellipsoids are drawn at the 50% probability level. c) 3D view of the crystal with hydrogen bonding (green dotted line). d) ORTEP view of **9** to show the cyclic geometry with the bridging water molecule. Thermal ellipsoids are drawn at the 50% probability level. All other atoms except the cycle are shown with 5% probability for clarity. Hydrogen atoms are also omitted for clarity.

a lattice of six perchlorate anions, two methanol molecules, and two water molecules. The geometry of the complex and the coordination environment of each copper ion are similar to those of complex **8**. Both copper ions form a distorted SP geometry with τ values of 0.388 and 0.436 for Cu1 and Cu2, respectively. Within the Cu1-(O1)-Cu2 core, the Cu···Cu distance is 4.463 Å and the Cu1-O-Cu2 bond angle is 137.92°. The bond angle of H-O-H in the bridging water molecule is 104.98° and the O–H bond length in the water molecule is 0.99 Å, similar to those of **8**. It was assumed that each NH_2 group of ethylamine from each peptoid ligand will bind the copper atom and will form a geometry similar to that of complex **7**. Surprisingly however, none of the NH_2 groups (N5 and N13) bind to Cu^{2+} because they are both protonated, probably because of their more basic nature (pK_a of R-NH_2 $\approx$ 35) compared with the OH groups (pK_a of R-OH $\approx$ 16). As a result, and to fulfill the pentacoordination geometry, the two Cu^{2+} ions in **9** are bridged by a H_2O molecule, similar to complex **8.** The two protonated NH_3^+ ions are neutralized by two perchlorate anions, which exist in the crystal structure of complex **9**, in addition to four more perchlorate anions that serve to balance the charge of the two Cu^{2+} ions.

Although all three complexes have cyclic structures, the oxo bridge between the two Cu^{2+} ions in **8** and **9** enables stacking of the aromatic rings, thereby leading to a unique assembly of the two peptoid chains in each complex. As a result, these two complexes adopt a very different shape compared to **7**. Thus, while complex **7** can be defined as a highly symmetric macrocycle, **8** and **9** can be described as the first examples of dinuclear double-stranded peptoid helicates (Figure 5). Overall, the formation of different structures from very similar peptoids demonstrates that

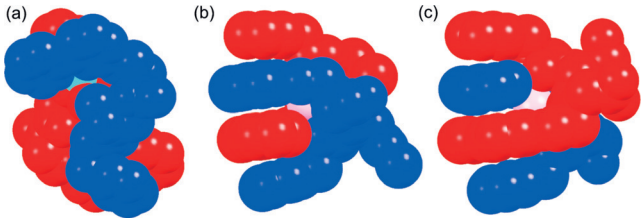

Figure 5. Representation of a) complex **7** and b) complex **8** and c) complex **9** with atoms represented as spheres. Each color indicates one binding peptoid.

minor sequence variations can lead to distinct assembly modes.

Similar to metallopeptoid **7**, complexes **8** and **9** have high solubility in acetonitrile and their dissolved crystals were also analyzed in solution. In the case of complex **8**, various MS studies revealed only traces of the macrocyclic (dipeptoid dicopper) complex with masses of 1214.9327 and 1216.9056, which correspond to the masses of **8** excluding the counterions (calcd Mw = 1214.32) and its protonated form, respectively (Figure S26). In contrast to **7** and **8**, however, similar measurements of complex **9** (calcd Mw = 1184.32) in acetonitrile disclosed a series of masses including 1223.9327, 1461.8342, 1563.2263, and 1662.4327 corresponding to the masses of $M+K^+$, $M+2K^++2ClO_4^-$, $M+2K^++3ClO_4^-$, and $M+2K^++4ClO_4^-$, respectively (Figure S27). The X-band EPR spectra of the dissolved crystals in acetonitrile solution, which was frozen at 180 K, clearly indicated the presence of Cu^{2+} ions in both metallopeptoids **8** and **9**. The Hamiltonian parameters obtained from simulation of the spectrum of **8** were $g_\parallel = 2.230$, $g_\perp = 2.075$, and $A_\parallel = 165$ G (Figure S28b) and those obtained from the simulated EPR spectrum of **9**, also measured from a frozen acetonitrile solution, were $g_\parallel = 2.224$, $g_\perp = 2.070$, and $A_\parallel = 164$ G (Figure S28c). These parameters can imply either a square-pyramidal geometry, as was seen in the crystal structure analysis, or a tetragonal $\{N_2O_2\}$ copper complex, as seen in the DFT calculations of **7** in solution.[24,10,15a] Overall, the spectroscopic data obtained for metallopeptoids **8** and **9** suggest that i) similar to **7**, macrocycle **8** is not stable in solution despite the additional oxygen bridge between the two copper ions, and ii) in contrast to **7** and **8**, complex **9** is present in solution. From these results it appears that the oxygen bridge alone does not play a crucial role in the stabilization of the macrocycles in solution and that another factor might control this stabilization. A key difference between the three structures is the intermolecular hydrogen bonding between the macrocycles and external stabilizing molecules. While **7** is stabilized by two interactions with perchlorate ions, **8** does not have such interactions at all and **9** is stabilized by four interactions, two with perchlorate ions, one with a water molecule, and one with methanol (see Table S4). The additional interactions in the case of **9** stem from the protonation of the two ethylamine groups to form ammonium cations, which are excellent hydrogen-bonding donors. Taken together we can propose that **9** is present in solution because it is stabilized by four intermolecular hydrogen-bonding interactions in addition to the internal

oxygen bridge between the two Cu^{2+} ions, while **7** and **8** are only stabilized by two such interactions or by the oxo bridge alone, respectively, which are not sufficient to retain the macrocyclic structures in solution. The observation that complex **9** is stable as a dimer in solution (in contrast to **7** and **8**, which are kinetically labile and undergo rapid ligand exchange), opens up new avenues for the design of functional metallopeptoids.

In summary, we disclose here the first three examples of self-assembled metallopeptoids and their unique crystal structures, and describe a distinctly new class of (self-assembled) metallo-peptidomimetics, two of which can be considered as the first dinuclear double-stranded peptoid helicates. The demonstration that two peptoid segments can self-assemble through metal coordination to create 3D structures is a milestone in the development of complex architectures from peptidomimetic scaffolds. Interestingly, solution studies and recrystallization of the dissolved crystals suggest that there exists a solid-state/solution equilibrium within this self-assembly process, which is a distinct biomimetic feature. Overall, our results represent a novel approach for the construction of unique Cu peptoids, and set the rules for their stabilization in solution. These structures represent new opportunities to generate high-order conformations as well as more complex and functional structures from metallopeptoids and other metallofoldamers on the one hand, and to explore metallo-peptidomimetics for various catalysis and recognition processes on the other.

Experimental Section

Crystallographic data were collected using a Nonius Kappa CCD and Bruker APEX-II/CCD diffractometer at 200 K with graphite-monochromated Mo-K_α radiation ($\lambda = 0.71073$ Å) and a cryostat system equipped with an N_2 generator. The crystals were removed from the solution, attached to a loop of nylon fiber with an antifreeze reagent (paraton-N, Hampton research), and mounted on a goniometer.

Crystal data for **7**: $C_{54}H_{64}Cu_2N_{12}O_{10}\cdot 4(ClO_4)\cdot 2(CH_3CN)\cdot 2(H_2O)$, $M_r = 1684.19$, triclinic space group $P\bar{1}$, $a = 11.2810(10)$, $b = 12.4220(10)$, $c = 14.8020(8)$ Å^3, $\alpha = 66.474(4)$, $\beta = 67.605(5)$, $\gamma = 86.129(4)°$, $V = 1749.6(2)$ Å^3, $Z = 1$, $\rho_{calcd} = 1.597\ g\,cm^{-3}$, $F(000) = 868$, $\theta_{max} = 24.72°$, $\mu = 0.856\ mm^{-1}$, reflections collected/unique 5960/4998 ($R_{int} = 0.0640$). 482 parameters, $R1 = 0.0617 (I > 2\sigma(I))$, $wR2 = 0.1312$. GOF = 1.107.

Crystal data for **8**: $C_{56}H_{70}Cu_2N_{12}O_{11},3(F_6P)\cdot ClO_4$, $M_r = 1748.66$, monoclinic space group $P21/c$, $a = 20.576(2)$, $b = 15.6734(18)$, $c = 21.976(3)$ Å^3, $\alpha = \gamma = 90$, $\beta = 93.040(3)°$, $V = 7077.5(14)$ Å^3, $Z = 4$, $\rho_{calcd} = 1.637\ g\,cm^{-3}$, $F(000) = 3552$, $\theta_{max} = 25.073°$, $\mu = 0.825\ mm^{-1}$, reflections collected/unique 12549/7557 ($R_{int} = 0.1330$). 984 parameters, $R1 = 0.0834 (I > 2\sigma(I))$, $wR2 = 0.2652$. GOF = 1.036.

Crystal data for **9**: $C_{54}H_{70}Cu_2N_{14}O_9,6(ClO_4)\cdot 2\,CH_4O\cdot 2\,H_2O$, $M_r = 1883.13$, monoclinic space group Pc, $a = 13.9867(9)$, $b = 23.2204(16)$, $c = 12.6143(8)$ Å^3, $\alpha = \gamma = 90$, $\beta = 92.9560(10)°$, $V = 4091.4(5)$ Å^3, $Z = 2$, $\rho_{calcd} = 1.523\ g\,cm^{-3}$, $F(000) = 1930$, $\theta_{max} = 25.042°$, $\mu = 0.811\ mm^{-1}$, reflections collected/unique 36354/12452 ($R_{int} = 0.0571$). 1068 parameters, $R1 = 0.0497 (I > 2\sigma(I))$, $wR2 = 0.1393$. GOF = 1.036.

CCDC 1559281, 1587088, and 1587089 (**7**–**9**) contain the supplementary crystallographic data for this paper. These data can be obtained free of charge from The Cambridge Crystallographic Data Centre.

Acknowledgements

This research was funded by the Solar Fuels Israel Center of Research Excellence (I-CORE) of the Israeli Science Foundation (ISF), grant number 2018762.

Conflict of interest

The authors declare no conflict of interest.

Keywords: copper coordination · foldamer · peptide · peptoid · self-assembly

How to cite: *Angew. Chem. Int. Ed.* **2018**, *57*, 7703–7708
Angew. Chem. **2018**, *130*, 7829–7834

[1] a) R. Zou, Q. Wang, J. Wu, J. Wu, C. Schmuck, H. Tian, *Chem. Soc. Rev.* **2015**, *44*, 5200–5219; b) J. J. Stephanos, A. W. Addison, *Chemistry of Metalloproteins: Problems and Solutions in Bioinorganic Chemistry*, Wiley, Hoboken, **2014**; c) R. H. Holm, P. Kennepohl, E. I. Solomon, *Chem. Soc. Rev.* **1996**, *96*, 2239–2314.

[2] a) T. Sawada, A. Matsumoto, M. Fujita, *Angew. Chem. Int. Ed.* **2014**, *53*, 7228–7232; *Angew. Chem.* **2014**, *126*, 7356–7360; b) S. Zhang, *Nat. Biotechnol.* **2003**, *21*, 1171–1178.

[3] a) W. Wang, Y. X. Wang, H. B. Yang, *Chem. Soc. Rev.* **2016**, *45*, 2656–2693; b) B. M. Schmidt, T. Osuga, T. Sawada, M. Hoshino, M. Fujita, *Angew. Chem. Int. Ed.* **2016**, *55*, 1561–1564; c) T. R. Cook, P. J. Stang, *Chem. Rev.* **2015**, *115*, 7001–7045; d) J. Rebek, *Angew. Chem. Int. Ed.* **2005**, *44*, 2068–2078; *Angew. Chem.* **2005**, *117*, 2104–2115; e) D. L. Caulder, K. N. Raymond, *Acc. Chem. Res.* **1999**, *32*, 975–982.

[4] a) J. D. Brodin, X. I. Ambroggio, C. Tang, K. N. Parent, T. S. Baker, F. A. Tezcan, *Nat. Chem.* **2012**, *4*, 375–382; b) S. Burazerovic, J. Gradinaru, J. Pierron, T. R. Ward, *Angew. Chem. Int. Ed.* **2007**, *46*, 5510–5514; *Angew. Chem.* **2007**, *119*, 5606–5610.

[5] a) N. A. Tavenor, M. J. Murnin, W. S. Horne, *J. Am. Chem. Soc.* **2017**, *139*, 2212–2215; b) M. Nepal, M. J. Sheedlo, C. Das, J. Chmielewski, *J. Am. Chem. Soc.* **2016**, *138*, 11051–11057; c) T. Sawada, M. Yamagami, K. Ohara, K. Yamaguchi, M. Fujita, *Angew. Chem. Int. Ed.* **2016**, *55*, 4519–4522; *Angew. Chem.* **2016**, *128*, 4595–4598.

[6] a) G. Guichard, I. Huc, *Chem. Commun.* **2011**, *47*, 5933–5941; b) D. Seebach, J. Gardiner, *Acc. Chem. Res.* **2008**, *41*, 1366–1375; c) S. Hecht, I. Huc, *Foldamers: structure, properties, and applications*, Wiley-VCH, Weinheim, **2007**; d) D. J. Hill, M. J. Mio, R. B. Prince, T. S. Hughes, J. S. Moore, *Chem. Rev.* **2001**, *101*, 3893–4011; e) S. H. Gellman, *Acc. Chem. Res.* **1998**, *31*, 173–180.

[7] a) G. Maayan, M. Albrecht, *Metallofoldamers. Supramolecular Architectures from Helicates to biomimetics*, Wiley, Hoboken, **2013**; b) G. Maayan, *Eur. J. Org. Chem.* **2009**, 5699–5710.

[8] a) M. Horeau, G. Lautrette, B. Wicher, V. Blot, J. Lebreton, M. Pipelier, D. Dubreuil, Y. Ferrand, I. Huc, *Angew. Chem. Int. Ed.* **2017**, *56*, 6823–6827; *Angew. Chem.* **2017**, *129*, 6927–6931; b) L. A. Churchfield, A. Medina-Morales, J. D. Brodin, A. Perez, F. A. Tezcan, *J. Am. Chem. Soc.* **2016**, *138*, 13163–13166; c) S. Tashiro, K. Matsuoka, A. Minoda, M. Shionoya, *Angew. Chem. Int. Ed.* **2012**, *51*, 13123–13127; *Angew. Chem.* **2012**, *124*, 13300–13304.

[9] a) M. Baskin, G. Maayan, *Biopolymers* **2015**, *104*, 577–584; b) T. Zabrodski, M. Baskin, P. J. Kaniraj, G. Maayan, *Synlett* **2014**, *25*, A–F; c) C. De Cola, G. Fiorillo, A. Meli, S. Aime, E. Gianolio, I. Izzo, F. De Riccardis, *Org. Biomol. Chem.* **2014**, *12*, 424–431;

d) G. Maayan, M. D. Ward, K. Kirshenbaum, *Chem. Commun.* **2009**, 56 – 58.
[10] M. Baskin, G. Maayan, *Chem. Sci.* **2016**, *7*, 2809 – 2820.
[11] J. P. Miller, M. S. Melicher, A. Schepartz, *J. Am. Chem. Soc.* **2014**, *136*, 14726 – 14729.
[12] a) R. Schettini, F. D. Riccardis, G. D. Sala, I. Izzo, *J. Org. Chem.* **2016**, *81*, 2494 – 2505; b) K. J. Prathap, G. Maayan, *Chem. Commun.* **2015**, *51*, 11096 – 11099; c) D. Chandra Mohan, A. Sadhukha, G. Maayan, *J. Catal.* **2017**, *355*, 139 – 144.
[13] G. Maayan, M. D. Ward, K. Kirshenbaum, *Proc. Natl. Acad. Sci. USA* **2009**, *106*, 13679 – 13684.
[14] a) T. M. Doran, M. Sarkar, T. Kodadek, *J. Am. Chem. Soc.* **2016**, *138*, 6076 – 6094; b) P. M. Levine, K. Imberg, M. J. Garabedian, K. Kirshenbaum, *J. Am. Chem. Soc.* **2012**, *134*, 6912 – 6915; c) N. P. Chongsiriwatana, J. A. Patch, A. M. Czyzewski, M. T. Dohm, A. Ivankin, D. Gidalevitz, R. N. Zuckermann, A. E. Barron, *Proc. Natl. Acad. Sci. USA* **2008**, *105*, 2794 – 2799.
[15] a) L. Zborovsky, A. Smolyakova, M. Baskin, G. Maayan, *Chem. Eur. J.* **2018**, *24*, 1159 – 1167; b) O. Roy, G. Dumonteil, S. Faure, L. Jouffret, A. Kriznik, C. Taillefumier, *J. Am. Chem. Soc.* **2017**, *139*, 13533 – 13540; c) B. C. Gorske, E. M. Mumford, C. G. Gerrity, I. Ko, *J. Am. Chem. Soc.* **2017**, *139*, 8070 – 8073; d) J. A. Crapster, I. A. Guzei, H. E. Blackwell, *Angew. Chem. Int. Ed.* **2013**, *52*, 5079 – 5084; *Angew. Chem.* **2013**, *125*, 5183 – 5188; e) J. R. Stringer, J. A. Crapster, I. A. Guzei, H. E. Blackwell, *J. Am. Chem. Soc.* **2011**, *133*, 15559 – 15567; f) K. Kirshenbaum, A. E. Barron, R. A. Goldsmith, P. Armand, E. Bradley, K. T. V. Truong, K. A. Dill, F. E. Cohen, R. N. Zuckermann, *Proc. Natl. Acad. Sci. USA* **1998**, *95*, 4303 – 4308.
[16] a) R. V. Mannige, T. K. Haxton, C. Proulx, E. J. Robertson, A. Battigelli, G. L. Butterfoss, R. N. Zuckermann, S. Whitelam, *Nature* **2015**, *526*, 415 – 420; b) K. T. Nam, et al., *Nat. Mater.* **2010**, *9*, 454 – 460.
[17] a) E. Macedi, A. Meli, F. De Riccardis, P. Rossi, V. J. Smith, L. J. Barbour, I. Izzo, C. Tedesco, *CrystEngComm* **2017**, *19*, 4704 – 4708; b) S. B. Y. Shin, B. Yoo, L. J. Todaro, K. Kirshenbaum, *J. Am. Chem. Soc.* **2007**, *129*, 3218 – 3225.
[18] R. N. Zuckermann, J. M. Kerr, S. B. H. Kent, W. H. Moos, *J. Am. Chem. Soc.* **1992**, *114*, 10646 – 10647.
[19] M. Baskin, L. Panz, G. Maayan, *Chem. Commun.* **2016**, *52*, 10350 – 10353.
[20] G. Maayan, L. K. Liu, *Pept. Sci.* **2011**, *96*, 679 – 687.
[21] a) *Comprehensive Coordination Chemistry*, *Vol. 5* (Eds.: B. J. Hathaway, G. Wilkinson, R. D. Gillard, J. A. McCleverty), Pergamon, Oxford, **1987**; b) A. W. Addison, T. N. Rao, J. Reedijk, J. van Rijn, G. C. J. Verschoor, *Dalton Trans.* **1984**, 1349 – 1356.
[22] D. L. Gerlach, I. Nieto, C. J. Herbst-Gervasoni, G. M. Ferrence, M. Zeller, E. T. Papish, *Acta Crystallogr. Sect. E* **2015**, *71*, 1447 – 1453.
[23] L. Öhrström, *Z. Krist. Cryst. Mater.* **2013**, *228*, III – IV.
[24] J. Peisach, W. E. Blumberg, *Arch. Biochem. Biophys.* **1974**, *165*, 691 – 708.
[25] a) K. Jayakumar, M. Sithambaresan, N. Aiswarya, M. R. P. Kurup, *Spectrochim. Acta Part A* **2015**, *139*, 28 – 36; b) K. A. V. Vologzhanina, S. V. Kats, L. V. Penkova, V. A. Pavlenko, N. N. Efimov, V. V. Minin, I. L. Eremenko, *Acta Crystallogr. Sect. B* **2015**, *71*, 543 – 554; c) K. Pagel, T. Ser, H. von Berlepsch, J. Griebel, R. Kirmse, C. Böttcher, B. Koksch, *ChemBioChem* **2008**, *9*, 531 – 536.
[26] G. F. Swiegers, T. J. Malefetse, *Chem. Rev.* **2000**, *100*, 3483 – 3537.

Manuscript received: January 15, 2018
Revised manuscript received: March 1, 2018
Accepted manuscript online: April 18, 2018
Version of record online: May 28, 2018

